

Study of Structural and Optical Properties of Ethylene - Vinyl Acetate Copolymer Films Irradiated with γ -Rays

F. H. Abd-El Kader *, G. Said , G. Attia and A. M. Abo-El Fadl
*Physics Department, Faculty of Science, Fayoum and *Physics Department, Faculty of Science, Cairo University, Giza, Egypt .*

THE INFLUENCE of γ -irradiation on X-ray diffraction, IR spectroscopy and UV-visible spectroscopy for ethylene-vinyl acetate copolymer (EVA) has been investigated. X-ray diffraction patterns of pristine and irradiated EVA samples have the same crystalline structure of polyethylene homopolymer. Samples irradiated with 5, 10, and 100 KGy γ -doses showed a maximum for both degree and index of crystallinity which are calculated from X-ray patterns and IR spectra respectively. The optical energy gaps and refractive indices of EVA samples at different γ -doses are also estimated. In addition, the calculated tristimulus, color indices and color scales are found to be γ -dose dependent.

Keywords: Copolymer; γ -ray; Energy gaps; Refractive index; Color parameters.

In recent years copolymers have attracted the attention of material researchers, with increasing interest for obtaining intermediate properties with respect to the homopolymers.

Optical properties of solids are directly related to the electronic structure like electrical properties^(1,2). In amorphous as in crystalline materials some useful information can be deduced both from absorption edge and infrared absorption spectral measurements, even though in such materials the edge is less sharp and the interaction peaks are broader than is normally the case of the crystals. Analysis of the absorption spectra in the lower energy part gives information about atomic vibrations, while the higher energy part of the spectrum ascertains inherent knowledge about the electronic states in the aggregate.

High-energy radiations, such as γ -rays, change the physical and chemical properties of the materials they pass through. Generally, the interaction of ionizing radiation with a polymer results in bonds rupturing and atomic displacement. These displaced atoms migrate through polymeric network until they are trapped somewhere in the lattice leaving deficiency regions. This in turn leads to the formation of color centers and modification of electronic structure of the polymer^(3,4).

The aim of the present work is to study the effects of γ -irradiation on the crystalline microstructure by X-ray diffraction and IR spectroscopy. In addition, UV/visible spectra are investigated to clarify the map of energy bands, optical constants and color of pristine and γ -irradiated EVA samples.

Experimental

The ethylene-vinyl acetate copolymer used in this work was kindly supplied by Hoechst Aktiengesellschaft, Frankfurt, Germany. The density of the material is $928 \pm 2 \text{ kg/m}^3$. Samples were irradiated by different doses of γ -rays in the range 1-100 kGy using ^{60}Co source with a dose rate of 8.6 kGy/hr at room temperature. X-ray diffraction patterns of the pristine and irradiated samples were performed using an advanced refraction system (Scintag / USA, Inc., Sunnyvale, CA). Infrared spectral analyses of the previous samples were performed using PYE Unicam spectrophotometer over the range of 400 - 4000 cm^{-1} . The ultraviolet / visible absorption spectra of the samples under investigation were recorded on a Berkin Elmer 4B spectrophotometer over the range 200-900 nm. The tristimulus transmittance values were calculated using the transmittance data obtained in the visible range according to CIE system⁽⁵⁾. Also, the color measurements such as: color scales (L^*, u^*, v^*), whiteness, yellowness (Y_e) and color difference (ΔE^*) were performed. All measurements were done 24 hr after irradiation.

Results and Discussion

1. X-Ray Diffraction

X-ray diffraction patterns of pristine and irradiated EVA samples in the range 5-100kGy γ -doses are shown in Fig.1. The X-ray spectra of irradiated samples are identical to that of pristine one. All spectra show a strong reflection peak at $2\theta = 19.98^\circ$ and two weak reflection peaks at $2\theta = 22.35^\circ$ and 34.89° , whose (hkl) planes are (110), (200) and (020) respectively^(6,7). Therefore, it is thought that copolymerization of ethylene and vinyl acetate does not have an effect on the structure of the polyethylene orthorhombic lattice^(6,8) and irradiation would only induce a minor change on the degree of crystallinity.

Resolution of crystalline peaks, together with an integration of the scattered intensities, provides a method for estimating of crystallinity. The degree of crystallinity (χ_c) is calculated according to the Hermans- Weidinger method⁽⁹⁾.

$$\chi_c = \frac{A(\text{crystalline})}{A(\text{crystalline}) + KA(\text{amorphous})} \quad (1)$$

where A (crystalline) and A (amorphous) are areas of crystalline reflections and amorphous halo, respectively; K is a constant and can be set to unity for comparative purposes. The calculated results for the irradiated EVA samples

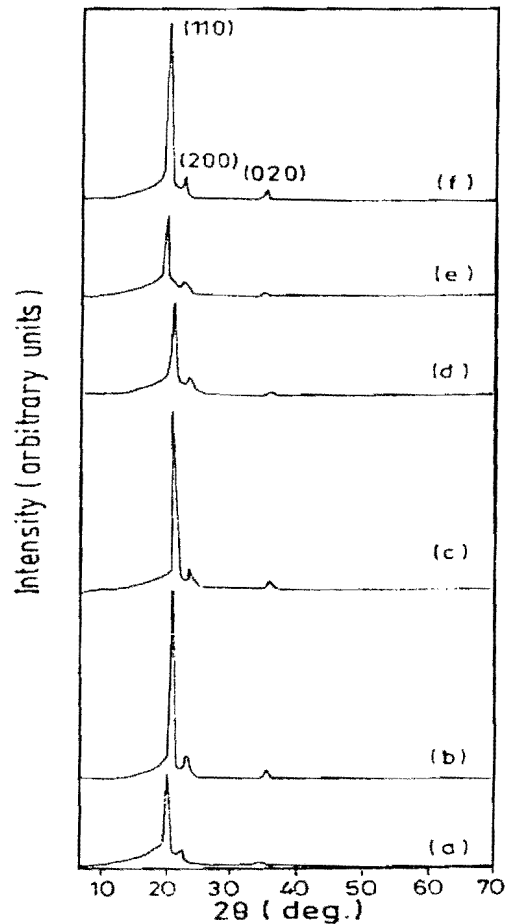


Fig. 1. X-ray diffraction patterns for (a) pristine EVA, (b) 5, (c) 10, (d) 20, (e) 50, and (f) 100 kGy irradiated EVA.

with 5, 10 and 100 kGy γ -doses have indicated an increase in the degree of crystallinity being 55.3 % ,53.8 % and 53.4 % respectively as compared to 42.3% for the pristine sample . It is believed that irradiation – induced scission of tout tie molecules permits recrystallization of broken chains from the noncrystalline regions resulting in an increase in the degree of crystallinity and an increased perfection of existing chain crystallites^(10,11) . However, a slight decrease in the degree of crystallinity values for irradiated samples with 20 and 50 kGy γ -doses has been noticed together with a small reduction in* the intensities of crystalline reflections. Radiation – induced crosslinking has been suggested to occur preferentially at the surfaces of folded chain lamellae or in the amorphous phase of bulk material and can cause stabilized chains , suppressed recrystallization of broken chains and crystal growth inhibition^(12,13) . These results agree well with many studies carried out to explore the location of crosslinking that occurs both in crystalline and amorphous regions, but predominantly in the latter region and in the interface between them^(14,15) . Therefore, it can be manifested that irradiation produces scission of tout tie molecules plus crosslinking in amorphous regions.

2. Infrared Spectra (IR)

The IR spectra and assignment of the most evident absorption bands for pristine EVA sample between 500 and 4000 cm^{-1} are illustrated in Fig. 2. Here, it appears that there is no appreciable difference in the absorption bands of EVA when compared with previously reported data⁽¹⁶⁾ except for the appearance of small intense absorption bands at (2019 & 1897 cm^{-1}) and (3500 & 608 cm^{-1}) for polyethylene and polyvinyl acetate (PVAc) contents respectively. Careful examination of the spectrum showed that the region of 2700-3100 cm^{-1} contains a large number of superimposed C-H absorption bands indicating the presence of a polymeric association of antisymmetric $\nu_{as}(\text{CH}_2)$ and symmetric $\nu_s(\text{CH}_2)$ stretching bands. The absorption band at 2019 cm^{-1} corresponding to methyl group stretching vibration $\nu(\text{CH}_2)$ is used as a reference peak, independent of the degree of crystallinity and oxidation^(15,17). The stretching band at 1897 cm^{-1} is known to be the crystallization- sensitive band of polyethylene^(18,19), while the band at 1298 cm^{-1} is associated with the amorphous region. The bands due to carbonyl stretch $\nu(\text{C}=\text{O})$ at 1740 cm^{-1} and carboxyl stretch $\nu(\text{C}-\text{O})$ at 1237 cm^{-1} are readily identifiable in the spectra. The bands at 1650 and 961 cm^{-1} are assigned to trans-vinylene double bond $\nu(\text{C}=\text{C})$. The bands at 1461 and 1370 cm^{-1} are due to methylene stretch $\nu(\text{CH}_2)$ in PE and methyl stretch $\nu(\text{CH}_3)$ in PVAc respectively. In addition, the 1139 cm^{-1} absorption band is assigned to $\nu(\text{C}-\text{C})$ stretching vibration. The band at 1015 cm^{-1} is associated with a C-O-C stretch mode while that at 727 cm^{-1} is assigned to $\nu_w(\text{CH})$ wagging vibration. Besides, the band at 609 cm^{-1} is related to $\nu_8(\text{O}-\text{C}-\text{O})$ bending vibration.

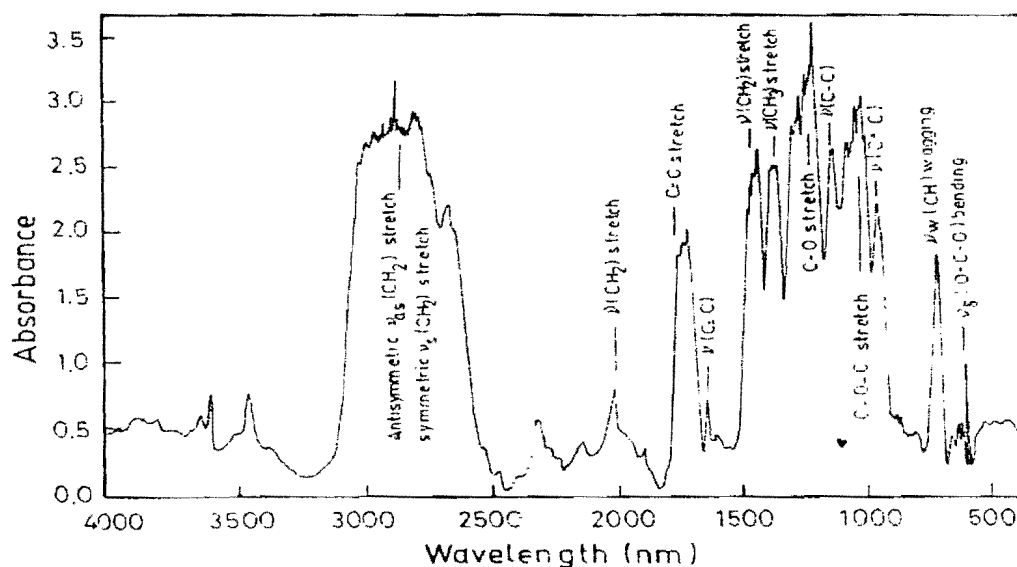


Fig. 2. Infrared spectra for pristine EVA .

The infrared spectra of pristine and irradiated EVA samples in the range of 5-100 kGy γ -doses are shown in Fig. 3 . In general, it appears from Figs. 2 and 3 that there is a significance difference between spectra of irradiated EVA samples at 5,10 and 100kGy γ -doses and pristine one. The bands at 1240, 1015 and 608 cm^{-1}

have disappeared in the spectra of irradiated EVA samples. The broad band of carbonyl group centered at 1740 cm^{-1} for pristine sample, which is due to the presence of polyvinyl acetate, shifts toward a lower frequency at about 1714 cm^{-1} and becomes a sharp band, which is attributed to keto – carbonyl group in the polyethylene. The band at 1714 cm^{-1} has also been observed previously in neutron and γ -radiolysis and is attributed to $\nu(\text{C}=\text{O})$ stretching owing to ketonic or acidic type carbonyl group^(20,21). The induced formation of the carbonyl group band at 1714 cm^{-1} can be interpreted on the basis of the peroxide – mediated oxidative degradation mechanism. γ -irradiation of the polymers results in bond cleavage giving free radicals that in the presence of oxygen react according to a chain mechanism to form oxidation products that include hydro – peroxides. The radical steps set in motion during the course of the reactions include pathways that lead to polymer chain scission and crosslinking. Also, it must be mentioned that the band at 720 cm^{-1} of irradiated samples is relatively broadened than the pristine sample.

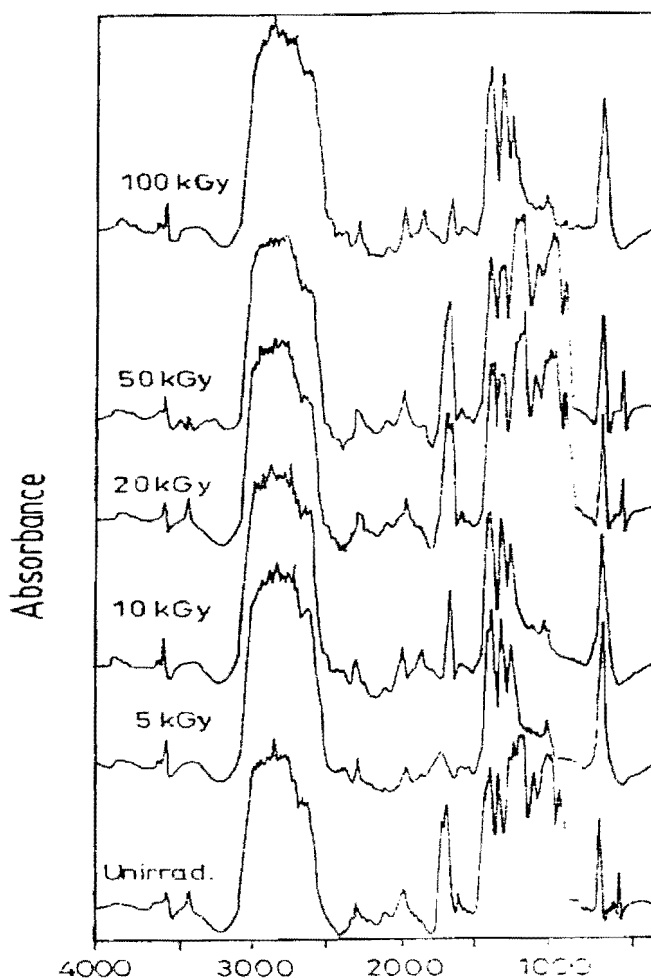


Fig. 3. IR spectra of pristine and irradiated EVA samples with different γ -doses.

On the other hand, there is no appreciable difference between the spectra of pristine and irradiated EVA samples at 20 and 50 kGy γ -doses apart from a very little change of intensity and position of the absorption bands. Radiolysis of polymers causes scission and/or crosslinking, the extent of which may change with the presence or absence of air. The irradiation conditions such as temperature, dose strength and phase relations in the polymers are of secondary importance, and their effect is not sufficiently known at the present time. Therefore, the similarity of IR spectra between pristine and irradiated EVA samples at 20 and 50 kGy γ -doses may be mainly due to the balanced effect of both crosslinking and degradation processes.

The index of crystallinity of the crystalline phase in pristine and γ -irradiated EVA samples can be calculated according to the following equation:

$$\text{crystallinity index (EVA)} = \frac{I(1897 \text{ cm}^{-1})}{I(2019 \text{ cm}^{-1})} \quad (2)$$

where $I(1897 \text{ cm}^{-1})$ and $I(2019 \text{ cm}^{-1})$ are the absorbance of crystallization sensitive band of EVA and the absorbance of reference band on the spectrum using the baseline method. The index of crystallinity is found to be 0.22 & 0.55, 0.59, 0.20, 0.21 and 0.50 (accuracy ± 0.01) for pristine and irradiated samples with 5, 10, 20, 50 and 100 kGy γ -doses respectively. The data reveal that the values of crystallinity index for irradiated EVA samples at 5, 10 and 100 kGy γ -doses is larger than the pristine one. On the other hand, the values of crystallinity index for irradiated EVA samples at both 20 and 50 kGy γ -doses is slightly less than the pristine sample. This agrees well with the results of X-ray diffraction patterns as discussed earlier.

3. UV / Visible Spectra

Figure 4 depicts the UV/visible spectra of pristine and irradiated EVA samples in the range 5-100 kGy γ -doses. The general characteristics of these spectra are composed of an almost flat baseline (negligible absorption) and a steep cut off (high absorption). The spectrum of pristine EVA sample shows a shoulder at 350 nm, which it may be due to $\pi \rightarrow \pi^*$ electronic transition (R-band) of chromophoric groups in PVAc. The spectra observed of irradiated EVA samples exhibit a new broad band, which position is irregularly changed with γ -doses in the range 240-280 nm. This band may be due to $\pi \rightarrow \pi^*$ electronic transition (K-band) of carbonyl groups formed from radiolatic oxidation of polyethylene by γ -rays. It is also relatively more pronounced at the 100 kGy γ -dose. This is probably due to the existence of free radicals eliminated during the presence of various environments as was previously detected in polyethylene⁽²²⁾. In addition, a shoulder at 350 nm for pristine sample has appeared with no observable change in the position but with small intensities at γ -doses 20 and

50kGy, while it disappeared at 5, 10 and 100 kGy γ - doses. The disappearance of the absorption shoulder at 350 nm may be due to modifications in molecular structure introduced as a result of the scission of side chain ester group in PVAc.

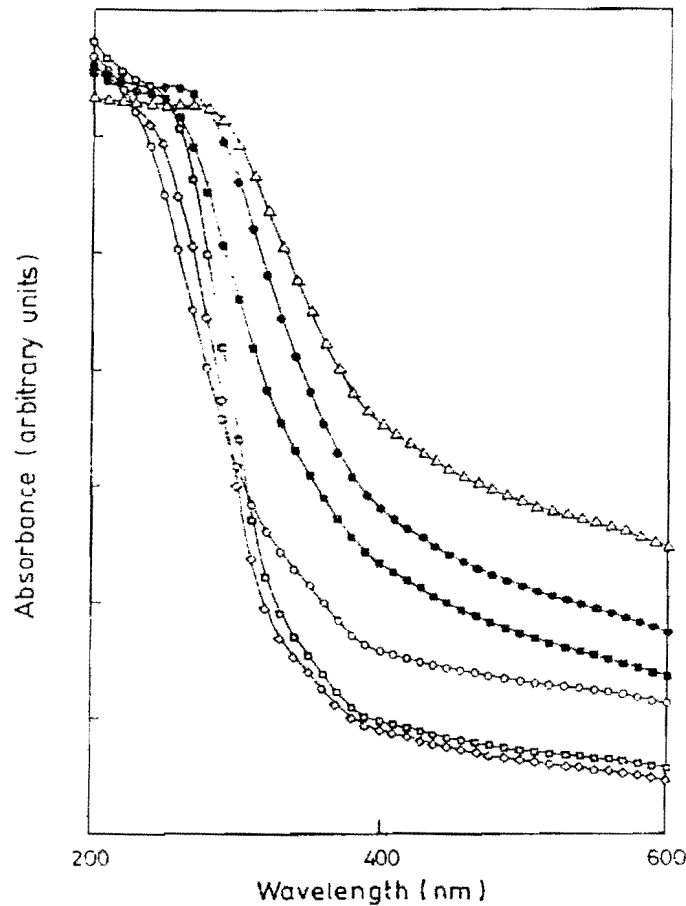


Fig. 4. Absorption spectra for EVA samples at different γ -doses, (o) pristine, (*) 5 kGy, (Δ) 10kGy, (\diamond) 20kGy, (\square) 50kGy, and (\bullet) 100kGy.

In general, it is obvious that the changes induced by γ -irradiation on spectral features in the UV/visible regions are compatible with that found in IR region.

4. Optical Parameters

Fundamental absorption edge

The absorption coefficient $\alpha(\nu)$ can be calculated from the optical absorption spectrum using the relation:

$$\alpha(\nu) = 2.303 A/d \quad (3)$$

where A is defined by $\log(I_0/I)$ where I_0 and I are the intensity of the incident and transmitted beams respectively and d is the film thickness in cm. The calculated values of absorption coefficient for pristine and irradiated EVA samples are relatively small ($20-90 \text{ cm}^{-1}$) as in most low carrier concentration semicrystalline materials. Thus, the films are weakly absorbing.

The fundamental absorption edge is one of the most important features of the absorption spectrum of a crystalline and amorphous materials. The increased absorption near the edge is due to the generation of neutral excitations and / or the transition of electrons from the valence band to the conduction band^(23,24). Fig. 5 shows the plot of absorption coefficient against photon energy for pristine and irradiated EVA samples. The $\alpha(\nu)$ exhibits a steep rise near the absorption edge and a straight line relationship is observed in the high α -region. The intercept of extrapolation to zero absorption with photon energy axis was taken as the value of absorption edge. Values of the absorption edge of the samples are represented in the inset of Fig.5 as a function of γ -dose . It is clear that the value of absorption edge decreases with increasing γ -dose up to 10 kGy, followed by an increase at 20kGy , and then it decreases slowly until 100 kGy . This may reflect the induced changes in the number of available final states according to γ -doses. The reduction of absorption edge at 5,10 and 100kGy compared to the pristine one can be attributed to the increase of crystallinity induced by γ -irradiation.

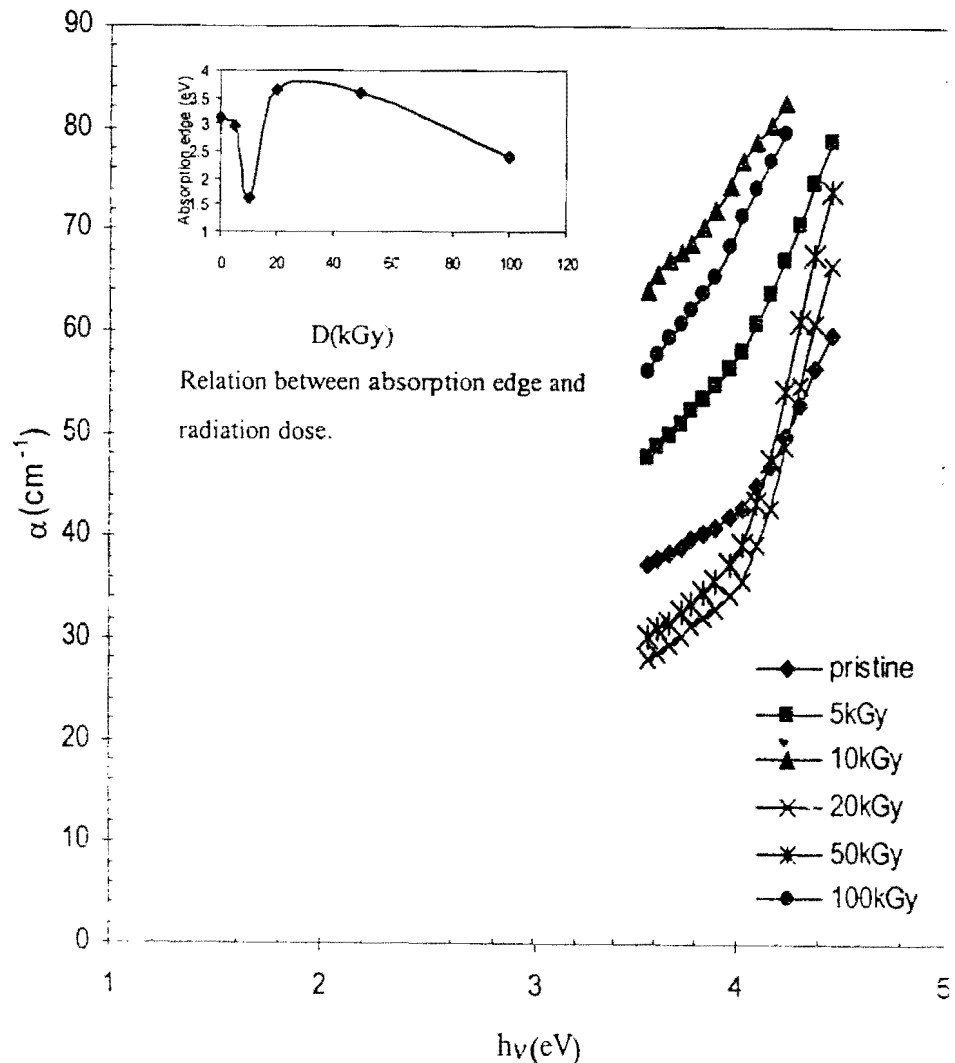


Fig. 5. Absorption coefficient as a function of photon energy $h\nu$ for EVA at different γ -doses. *Egypt. J. Phys.* Vol. 37, No. 2 (2006);

Optical band gaps

The fundamental absorption is related to band to-band (excitons) transitions, and are subject to certain selection rules⁽²⁵⁾. The allowed direct and indirect transitions are given by :-

$$\alpha h\nu = A (h\nu - E_{gd})^{1/2} \quad (4)$$

$$\alpha h\nu = B \left[\frac{(h\nu - E_{gi} + E_p)^2}{\exp(E_p/kT) - 1} + \frac{(h\nu - E_{gi} - E_p)^2}{1 - \exp(-E_p/kT)} \right] \quad (5)$$

where A and B are constants, E_{gd} and E_{gi} are the direct and indirect energy gaps respectively and E_p is the phonon energy. From eqns.(4)&(5) by plotting $(\alpha h\nu)^2$ and $(\alpha h\nu)^{1/2}$ against $h\nu$, the values of E_{gd} , E_{gi} and E_p could be deduced for pristine and irradiated samples (Figs. not shown). These values are listed in Table 1, within an accuracy of ± 0.02 eV.

TABLE 1. Values of band tails, optical energy gaps, and phonon energy of EVA samples at different γ -doses.

Dose (kGy)	E_{gd} (eV)	E_{gi} (eV)	E_p (eV)	E_c (eV)
0	3.82	2.89	0.40	1.24
5	3.78	2.75	0.33	1.43
10	3.33	2.15	0.31	2.50
20	4.01	3.32	0.37	0.64
50	3.97	3.20	0.36	0.67
100	3.49	2.57	0.21	1.90

It is clear that the values of E_{gd} & E_{gi} decrease with increasing γ -dose up to 10kGy, followed by an increase at the dose 20 kGy, and then decreases again until 100 kGy. The influence of γ -irradiation can be explained in terms of diminution of disorder, defects in the structural bonding and crystal field mechanism⁽²⁶⁾.

In the mean time, the absorption tails in amorphous and semicrystalline materials could be interpreted in terms of the Dow-Redfield effect⁽²⁷⁾ taking the form of Urbach rule⁽²⁸⁾ as follows:

$$\alpha(h\nu) = \alpha_0 \exp(h\nu/E_c) \quad (6)$$

where α_0 is a constant and E_c is the width of the tail of the localized states in the band gap. Plotting $\ln(\alpha)$ against $h\nu$ for present EVA sample before and after irradiation yield values of band tails E_c , as indicated in Table 1. The appearance of band tails is due to disorder in the system⁽²⁹⁾ and its broadening is caused by morphological changes upon irradiation according to a compromise between the degradation and crosslinking processes^(30,31). Also, the reduction of the direct and

indirect band gap energies at 5, 10 and 100 kGy γ -doses compared to the pristine sample could be attributed to the increase of tailing into the gap. The tail increase is a result of the increase in the number of unsaturated defects due to γ -rays, consequently increase the density of localized states in the band structure leading to a decrease in the optical energy gap.

Optical constants n and k

The optical behavior of a material is generally characterized by its optical constants, n and k where n is the refractive index and k is the extinction coefficient. The extinction coefficient can be obtained from the absorption coefficient using the expression $k = \alpha\lambda / 4\pi$. The values of k for pristine and irradiated EVA samples are found small in the order 10^{-5} throughout the studied wavelength range, indicating that the investigated samples are insulators⁽³¹⁾ without defects⁽³²⁾.

If multiple reflections are neglected, reflectance R of the samples can be calculated from the experimentally measured values of transmittance T (Figs. not shown) and absorbance using the following equation:

$$R = 1 - [T \exp(\alpha d)]^{1/2} \quad (7)$$

Using the values of k and R , the refractive index can be determined from the following equation:

$$n = [(1+R) / (1-R)] \pm \{[(R+1) / (R-1)]^2 - (1+k^2)\}^{1/2} \quad (8)$$

Reasonable values for n may be evaluated by considering the plus sign of eqn. 8.

Figure 6 shows the $n(\lambda)$ characteristics from 450 nm to 800 nm for pristine and irradiated EVA in the range 5 to 100 kGy γ -doses. It is clear that the refractive index at 5, 10 and 100kGy irradiated samples are higher than pristine sample, while the refractive index values at 20 and 50kGy irradiated samples are very close to the pristine one. In general, the refractive index increases slightly with decreasing wavelength, and changes become larger at shorter wavelengths showing the typical shape of a dispersion curve. But, the rate of increase of refractive index with decreasing wavelength is appreciably high for the 5, 10 and 100kGy irradiated samples as compared to the other irradiated samples and the pristine one. This relatively big increase of refractive index in the region 450-650 nm may be attributed to an increase in the density of current carriers in the valance band.

The changes of refractive index could be due to different factors such as the crystallinity, density, electronic structure and defects. Therefore, the variation in the refractive index values of the irradiated samples can be attributed to varying electronic structure and crystallinity induced by γ -irradiation depending upon whether degradation or crosslinking process is predominant.

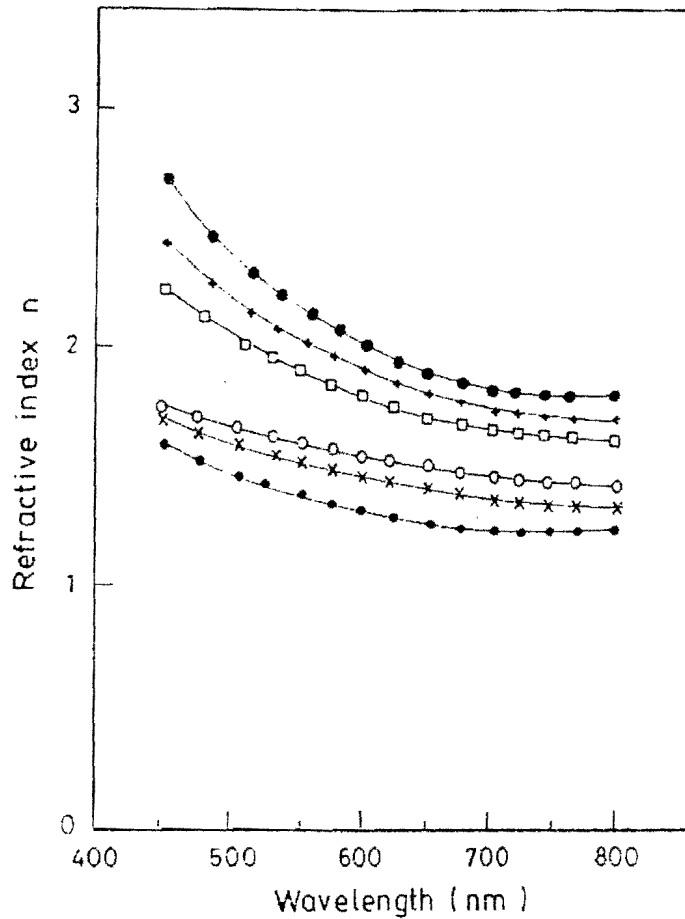


Fig. 6. Variation of refractive index with wavelength at different γ -doses: (o) pristine, (□) 5kGy, (+) 10kGy, (·) 20kGy, (x) 50kGy, and (●) 100kGy for EVA.

Color Difference Calculations

Various classification systems have been proposed for the description of a colored object. One of these is the CIEXYZ which is internationally recognized. Any color is specified by its tristimulus values XYZ depending on the color matching functions of the standard observer defined by the CIE⁽³²⁾.

Figure 7 illustrates the variation of the tristimulus transmittance values (y_i) with wavelength in the range 380-760 nm for pristine and irradiated EVA samples. It is noticed that the behaviors of y_i for all samples are similar and have the same peak position at about 560 nm. The inset of Fig. 7 shows the dependence of y_i at the peak position (560 nm) as a function of γ -doses for EVA copolymer. It is clear from the inset that $y_i(\text{max})$ at 5, 10 and 100 kGy irradiated samples are lower than pristine sample, while $y_i(\text{max})$ at 20 and 50 kGy irradiated samples are higher than the pristine one. These changes reflect the damaged sites and the color center creations in the irradiated material.

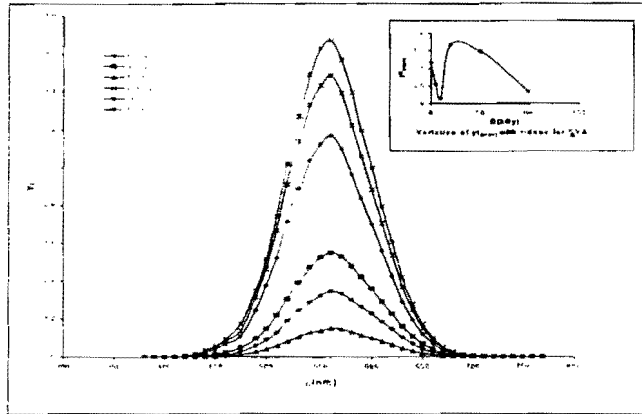


Fig. 7. Variation of the tristimulus transmittance value with wavelength λ for EVA at different γ -doses.

The chromaticity coordinates x and y defining the position of the specimens on the chromaticity locus and their distances to the white point have been calculated for pristine and irradiated EVA samples and are depicted in Fig. 8. A great similarity exists between zero, 20 and 50kGy irradiated specimens and also between 5, 10 and 100kGy irradiated specimens, so that each group is overlapped and represented by a single point.

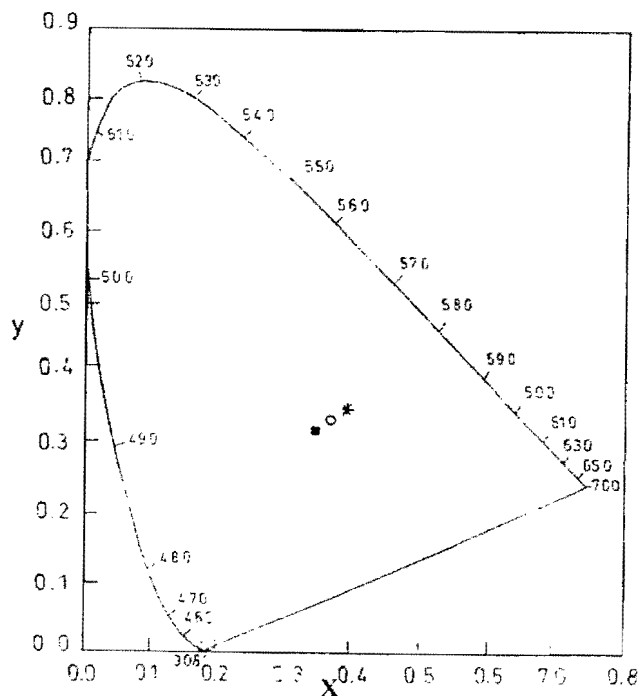


Fig. 8. Chromaticity diagram of pristine and irradiated EVA : (*)0,20 and 50 kGy (*) 5,10 and 100 kGy .

Table 2 represents the variation of color parameters (L^* , Δu^* , Δv^* , ΔC^* , h° , ΔE^* , W and Ye) of EVA as a function of γ -dose calculated from the transmittance data. The values of L^* (lightness) and h° (hue) for irradiated EVA samples at 5,10 and 100kGy γ -doses are lower than the value of pristine sample. On the other hand, these values for irradiated samples at 20 and 50 kGy γ -doses are higher than the value of pristine sample. This indicates that the irradiated samples at 5,10 and 100 kGy γ -doses are darker and more reddish yellow while the irradiated samples at 20 and 50 kGy γ -doses are lighter and less reddish yellow in comparison to pristine one.

TABLE 2. The results of color parameters for EVA calculated from the transmittance curves.

γ -dose (kGy)	L^*	Δu^*	Δv^*	ΔC^*	h°	ΔE^*	W	Ye
0	34.90	-	-	-	56.60	-	-141.60	0.25
5	23.60	2.53	3.68	4.46	56.20	12.16	-66.70	0.55
10	9.61	-1.55	-2.58	-3.00	55.30	25.48	-18.04	0.57
20	41.30	0.99	2.14	2.34	58.45	6.86	-202.50	0.27
50	39.10	0.21	0.74	0.74	58.03	4.28	-179.80	0.26
100	17.70	1.35	1.16	1.73	53.84	17.26	-41.30	0.58

L^* (lightness) Δu^* (red – green) Δv^* (yellow – blue) ΔC^* (chroma difference)

h° (hue) ΔE^* (total color differences) W (whiteness index) Ye (yellowness index)

To assess the coloration effects of the samples, Δu^* (red-green), Δv^* (yellow-blue) and total ΔE^* color differences in addition to ΔC^* chroma difference of irradiated samples with respect to the pristine one were calculated. The values of Δu^* , Δv^* color and chroma differences ΔC^* are positive for all irradiated samples except for the sample irradiated at 10 kGy γ -dose is negative. Thus, the 10 kGy irradiated sample is more green, more blue and less saturated than the pristine one. However, the irradiated samples at all other γ -doses are more red, more yellow and more saturated than the pristine one. In addition, the total color difference ΔE^* apparently attain values such that at 10kGy > 100kGy > 5kGy > 20kGy > 50kGy.

The whiteness index data W in Table 2 indicate that EVA samples irradiated with 5, 10 and 100kGy γ -doses have higher values than the pristine sample. On the contrary, the irradiated samples with 20 and 50 kGy γ -doses are less than the pristine sample. The yellowness index values (Ye) increase for irradiated samples except for 20 and 50kGy γ -doses have nearly the same value of pristine sample.

It may be presumed that the effect of γ -radiation on EVA copolymer is the destruction of the chemical bonds and linkages as well as creation of highly energetic electrons and ions⁽³³⁾. These highly energetic species migrate in the plastic network causing further damage to the adjacent macromolecules through their tracks and may be trapped somewhere in the network forming color centers.

The degree of variation in the color parameters depends on the total quantity of γ -radiation energy received by the material⁽³⁴⁾.

Conclusion

- 1-The crystallinity data resulting from X-ray patterns and IR spectra reveal that the γ -irradiated EVA samples at 5,10,and 100 kGy possess larger crystallinity values as compared to the pristine one , while those irradiated with 20 and 50 kGy exhibited lower crystallinity values .
- 2-From UV/visible studies, it is recognized that γ -irradiation highly affect the electronic structure and molecular configuration of the polymer matrix . This is clearly shown by the pronounced change in the absorption spectra and is confirmed by optical parameters obtained for the samples under investigation.
- 3- The reduction of absorption edge at 5,10,and 100 kGy irradiated EVA samples than the pristine one can be attributed to the increase of crystallinity induced by γ -irradiation ,which is consistent with IR and X-ray diffraction data .

References

1. Yakuphanoglu, F., Erol, I. , Aydogdu, Y. and Ahmedzade, M., *Mat. Lett.*, **57**, 229 (2002).
 2. Vijayalakshmi Rao, R. and Shridhar, M. H. , *Mat. Chem. and Phys.* , **76** , 171 (2002).
 3. Lim, S. L. , Fane, A. G. and Fell, C. J. , *J. Appl. Polym. Sci.* , **41** , 1605 (1990).
 4. Chu, K. C. , Jordan, K. J. Battista, J. J. Van-Dyk, J. and Rutt, B. K. , *Phys. Med. Biol.* , **45**, 955 (2000).
 5. MacAdam, D. L., "*Color Measurements Theme and Variation*", Springer, Heidelberg (1981).
 6. Ikada, Y., Nakamura, K., Ogata, S., Makino, K., Tajima, K., Endoh, N., Hayashi, T. , Fujita, S. , Fujisawa, A. , Masuda, S. and Oonishi, H. , *J. Polym. Sci. Part A: Polym. Chem.*, **37**, 159 (1999).
 7. Baker, A. M. E. and Windle, A. H. , *Polymer*, **42** , 681 (2001).
 8. Schwartz, K. W. and Con Dreck, R. B. , *Adv. X-Ray Anal*, **39** , 515 (1997).
 9. Hermans, P. H. and Weidinger, A. , *Makromol. Chem.* , **44**, 24 (1961), **50**, 98 (1961).
 10. Shinde, A. and Solovey, R. , *J. Polym. Sci. Part B: Polym. Phys.*, **23**, 1681 (1985).
 11. Minkova, L., *Colloid Polym. Sci.*, **266** , 6 (1988).
- Egypt. J. Phys.* Vol. 37, No. 2 (2006)

12. Dole, M. , *Polym. Plast. Technol. Eng.*, **13** ,41 (1979).
13. Ungar, G. , *J. Mat. Sci* , **16** , 2635 (1981).
14. Dole, M. , Gupta, C. and Guezdic, N. , *Phys. Chem.* , **14**, 711 (1979).
15. Luo, Y. , Wang , G. , Lu, Y. , Chan, N. and Jiong, B. , *Radiat. Phys. Chem.* , **25**, 399 (1985) .
16. Rubb, D. M. , McGill, R. A. , Horwitz, J. S. , Fitz-Gerald, J. M. , Houser, E. J., Stroud, R. M. , Wu, P. W. , Ringeisen, B. R. , Pique', A. and Chrisey, D. B. , *J. Appl. Phys.* , **89** , 5739 (2001) .
17. Lambert, J.B., Shurvell, H.F., Lightner, D.A. and Cooks, R.G., "*Organic Structural Spectroscopy*" , Prentice Hall Inc. , New York (1998) .
18. Dietl, J.T. , *Kanstoffe* , **59** , 515 (1961) .
19. Billmeyer , F. W. , Jr : "*Text Book of Polymer Science*" , Wiley Intersci. Pub. , New York (1971).
20. Abd El-kader, F. H., Gaafar, S. A., Rizk, M. S. and Kamel, N. A. , *J. Appl. Polym. Sci.* , **72** , 1395 (1999).
21. Buchanan, F. J. , Whith, J. R. , Sim, B. and Downes, S. , *J. Mat. Sci. : Mat. in Med.* , **12**, 29 (2001).
22. Bodily, D. M. and Dole, M. , *J. Chem. Phys.* , **45** , 1428 (1967) .
23. Miller, A. , " *Handbook of Optics* " , Vol.1, Chap. 9 , McGraw Hill , New York (1994) .
24. Abd El-kader , F. H. , Osman, W. H. , Ragab, H. S. , Shehap . A. M. , Rizk, M. S. and Basha, M. A. F. , *J. Polym. Mater.*, **21** ,49 (2004) .
25. Pankove , J.I. , "*Optical Processes in Semiconductors*" , Prentice Hall , NJ (1972) .
26. Chaudhuri, S. , Biswas, S. K. and Choudhury, A. , *J. Mater. Sci.* , **23** , 4470 (1988)
27. Dow, J. and Redfield, D. , *Phys. Rev. B*, **8** , 3358 (1970).
28. Urbach, F. , *Phys. Rev.* , **92**, 1324 (1953).
29. Davis, E. A. and Mott, N. F. , *Phil. Mag.*, **22** , 903 (1970).
30. Osman, W. H. , *J. Mat. Sci. : Materials in Electronics* , **8** , 57 (1997)
31. EL-Sayed, S.M. , Arnaouty, M.B. and Fayek, S.A. , *Polymer Testing*, **22**, 17 (2003).
32. CIE, Publication No. 15.2, *Colorimetry*, 2nd Ed., Commission Internationale de'Eclairage, Vienna, Austria (1986) .

33. Ludosik, D. and Macko, P. , *J. Non-Cryst. Solids* , **44** , 397 (1981).
34. Parkinson, W.W. , " *Encyclopedia of Polymer Science and Technology* " , Vol II , Bikals , N. M. , Mark, H. F. and Goylard, N. G. , John Wiley , NY (1969) .

(Received 9/2/2005;
Accepted 23/4/2005)

دراسة الخواص التركيبية والضوئية للبوليمر الإسهمي (بولي إيثيلين - بولي فينيل اسيتيت) المشع بأشعة جاما

فوزى حامد عبد القادر* - جمال سعيد - جمالي عطيه و عزه محرم أبو الفضل
قسم الفيزياء -- كلية العلوم- الفيوم و قسم الفيزياء - كلية العلوم - جامعة
القاهرة - الجيزة - مصر .

يتناول هذا البحث دراسة تأثير أشعة جاما على كل من حيود الأشعة السينية ، و الأطياف الضوئية في نطاقى الأشعة فوق البنفسجية و الأشعة تحت الحمراء للبوليمر الأسهمى (بولى إيثيلين - بولى فينيل اسيتيت) و لقد أظهرت دراسة حيود الأشعة السينية أن العينات غير المشعة و المشعة لها نفس التركيب البلورى للبوليمر بولى إيثيلين المنفرد . كما وجد أن العينات المشعة بجرعات ٥ ، ١٠ ، و ١٠٠ كيلو جراى تعطى أعلى قيمة لكل من درجة و معامل التبلور المحسوبة من خلال الأشعة السينية و الأشعة تحت الحمراء على التوالى .

بعد ذلك تم حساب كل من فجوة الطاقة ، الطاقة الممتدة للنطاق و معامل الانكسار للمركب قبل و بعد التشعيع. بالإضافة إلى ذلك دلت نتائج معاملات اللون اعتمادها على الجرعات الأشعاعية .